Hindawi
Shock and Vibration
Volume 2019, Article ID 6571896, 10 pages
https://doi.org/10.1155/2019/6571896

Research Article

Bending Vibration Analysis of Tensioned Ball Screw under Nonuniform Stress during the Cutting Process

Cheng Zhang and Jianrun Zhang

School of Mechanical Engineering, Southeast University, Nanjing 211189, China

Correspondence should be addressed to Jianrun Zhang; zhangjr@seu.edu.cn

Received 5 September 2018; Revised 3 March 2019; Accepted 10 March 2019; Published 21 March 2019

Academic Editor: Francesco Franco

The bending vibration of tensioned ball screw under nonuniform stress in the cutting process is analyzed in this paper. Differential equation of a beam under nonuniform prestress is derived according to Euler–Bernoulli beam theory. A method to solve the differential equation under different boundary conditions is proposed based on the segmentation method. The correctness of the method is verified by comparison with the traditional method and experiment, respectively. The dynamic analysis of tensioned ball screw under nonuniform stress in the cutting process is carried out with this method. The influence of the location on the ball screw and amplitude of the axial force produced in the cutting process on natural frequencies of ball screw is researched. Results show that the greater the force, the greater the change in natural frequencies. Furthermore, the change of first two natural frequencies presents a simple harmonic trend with the force moving along the ball screw. Taking a set of cutting force data as an example, the instantaneous frequency of tensioned ball screw in the cutting process is calculated in the end.

1. Introduction

Ball screw feed drives are widely used in machine tools due to their high stiffness and accuracy. The positioning accuracy and speed directly determine the quality and productivity of machine tools [1]. For the speed-up of machine tools, the ball screw feed drives operate at high speed, which leads to the increase of vibration and position errors [2]. Hence, it is necessary to study the dynamic characteristics of ball screw feed drives.

In recent decades, scholars have done a lot of research on the vibration characteristics of ball screw. Dynamic modeling of the ball screw feed drive system is one of the important research contents. Choi et al. [2] proposed a 6 degree-of-freedom lumped parameter model in order to investigate the dynamic characteristics of ball screw feed drive system. Zhang et al. [3] proposed an analytical modeling approach of ball screw feed drive system modeled by a mass-spring system. With this approach, the dynamic behavior of the feed drive system could be proposed. Based on the system modeling methods, some scholars have studied the influence of some factors on the dynamic performance of the system. Wang et al. [4] studied the effect of stiffness of rolling joints on vibrations of ball screw feed drive system in a milling machine by numerical calculation. Jiang and Zhu [5] built a dynamic model of linear guideway joint with ball screw and analyzed the influence of cutting load on the dynamic stiffness of joint part. Hung et al. [6, 7] considered the preload of linear guides in the ball screw feed drive and analyzed the dynamic behavior of a vertical column-spindle system. The modeling methods are also used for error compensation. Huang et al. [8] and Li et al. [9] proposed the dynamic models to derive the elastic deformation of the feed drive system. Then, the results were used to offset the position commands that are fed to the servo controller. Although these studies have researched the dynamic characteristics of the ball screw feed drive system, most of them do not consider the influence of prestress on the dynamic performance of the ball screw.

In fact, prestress has a certain effect on the dynamic characteristics of some structures, especially plates and beams. Bideau et al. [10] researched the modal of shearable beams with initial finite strain and found that the frequency increased with prestress. Ashwear and Eriksson [11] studied the natural frequencies of the tensegrity structures with prestress. Using the Euler–Bernoulli beam element, the stiffness matrix and the mass matrix were formulated. It was found that the natural frequencies may rise or fall when the level of prestress increased for a certain tensegrity structure. Nieves et al. [12] studied the nonlinear bending vibration of a thick plate subjected to axial forces with the employment of the theory of nonlinear deformation. These research studies mainly considered the influence of the uniform prestress on the dynamic performance of structures. In order to analyze the influence of complex prestress distribution on structural dynamic performance, some finite element methods (FEM) considering prestress are proposed. Kashani et al. [13] developed the dynamic finite element method to analyze the prestressed, bending-torsion coupled beams. Zhang et al. [14] adopted the prestressed component mode synthesis method to optimize the mistuned bladed disk considering the prestress. Li et al. [15] put forward a prestressed component modal synthesis superelement method for vibration analysis of aeroengine blisk structure. The accurate results can be obtained with FEM when enough elements are established. However, the calculation difficulty is relatively great [14]. Meanwhile, the FEM considering the prestress is difficult to analyze. Some scholars established differential equations of the structures with complex prestress distribution to conduct the dynamic analysis. Li and Chen [16] researched the top-tensioned rider in consideration of complex prestress distribution. The differential equation of the rider with complex prestress distribution was established, and Galerkin's procedure was employed to solve the equation. However, the boundary condition at both ends of the rider was modeled as simple support which was not applied to all structures. Li [17] introduced a new analytical method of instantaneous frequency based on experimental data, namely, the Hilbert–Huang transform method. An experiment was carried out with a simply supported beam, and the data were analyzed in the basis of fast Fourier transformation and Hilbert–Huang transform methods, respectively. Because prestressing can increase natural frequency, it is applied in some aspects. Zhang et al. [18] experimentally found that tension force can effectively enhance the stiffness and natural frequency of blade-fixture system. Based on this result, Wan et al. [19] proposed a method to improve chatter stability of thin-wall milling by prestressing.

In order to compensate for the axial elastic deformation in machining, the ball screw is generally assembled by pretension. Therefore, the ball screw is uniformly prestressed, which may influence the dynamic characteristics of the ball screw according to existing research. Moreover, there is axial force applied on the ball screw, and the force varies in the cutting process. As a result, the ball screw is subjected to nonuniform stress in the process of machining.

In this paper, bending vibration of tensioned ball screw under nonuniform stress is analyzed. A method to analyze the dynamic characteristics of the nonuniformly prestressed beam under different boundary conditions is proposed. The frequencies of a simply supported beam subjected to axial uniform prestress are calculated on the basis of the method proposed in this paper and the traditional method, respectively. Moreover, a comparison between the proposed method and an experiment is carried out. The correctness of the method proposed in this paper is then verified. The bending vibration of tensioned ball screw is analyzed with this method, and the effects of the location and amplitude of the axial force on frequency are investigated. At last, a set of cutting force data is taken as an example to calculate the instantaneous frequency of the tensioned ball screw during the cutting process. These findings can provide the guidance for the design and installation of ball screws and machine tools. The dynamic characteristics of other nonuniformly prestressed beams can also be analyzed based on the method proposed in this paper.

2. Bending Vibration of a Beam Subjected to Nonuniform Prestress

The ball screw is subjected to nonuniform stress during processing by simple analysis. In order to analyze the dynamic characteristics of the ball screw, bending vibration analysis of a beam subjected to nonuniform prestress is carried out.

As is known to all, the motion differential equation of beam bending vibration is as follows when damping is not considered:

$$EI\frac{\partial^4 w}{\partial x^4} + \rho A\frac{\partial^2 w}{\partial t^2} = F(t), \tag{1}$$

where E is Young's modulus, I is the moment of inertia of cross section, ρ is the density, A is the cross section area of the beam, w is the transversal displacement, x is the axial coordinate, t is the time, and $F(t)$ is the external force. In this paper, the influence of the nonuniform distribution of axial stress is mainly considered, so only the equal-section beam is analyzed, i.e., I and A are constants.

When the beam is subjected to a nonuniform prestress distribution, the free vibration differential equation can be derived as

$$EI\frac{\partial^4 w(x,t)}{\partial x^4} + \rho A\frac{\partial^2 w(x,t)}{\partial t^2} - A\cdot\sigma(x)\frac{\partial^2 w(x,t)}{\partial x^2} = 0, \tag{2}$$

where $\sigma(x)$ is the cross section stress distribution function of the beam.

By using variable separation, the solution of equation (2) can be set as follows:

$$w(x,t) = W(x)\left(U_1\cos\omega t + U_2\sin\omega t\right), \tag{3}$$

where $W(x)$ is the vibration mode function, U_1 and U_2 are constants, and ω is the natural frequency.

The modal differential equation can be obtained by substituting equation (3) into equation (2), which is shown as follows:

$$EI\frac{d^4W(x)}{dx^4}-\omega^2\rho A\cdot W(x)-A\cdot\sigma(x)\frac{d^2W(x)}{dx^2}=0. \quad (4)$$

In order to solve equation (4), the solution of equation (4) is set as

$$W(x)=U_3e^{sx}. \quad (5)$$

When the beam is axially uniformly prestressed, $\sigma(x)=\sigma_0$ is a constant. Then, the root of the equation can be obtained as follows:

$$s_1^2,s_2^2=\frac{\sigma_0A}{2EI}\pm\sqrt{\left(\frac{\sigma_0A}{2EI}\right)^2+\frac{\rho A\omega^2}{EI}}, \quad (6)$$

where s_1 is a real number and s_2 is an imaginary number.

Then, the vibration mode function $W(x)$ can be expressed as the following trigonometric function according to equations (5) and (6):

$$W(x)=a\cosh s_1x+b\sinh s_1x+c\cos is_2x+d\sin is_2x, \quad (7)$$

where a, b, c, and d are the coefficients and i is the imaginary unit, $i^2=-1$.

Therefore, when the beam is subjected to axial uniform prestress, i.e., as a constant, the corresponding natural frequency and vibration mode function can be obtained according to equations (6) and (7).

However, in practical engineering, there may be nonuniform stress distributions in the beam structure. The simple stress distribution form, such as ball screw, has different stresses in the two segments of the ball screw separated by the point of force in machining. The complex stress distribution form, such as welding beam structure, may have a continuously changing stress distribution. So, the application range of the vibration mode function obtained in equation (7) is very limited. Nevertheless, equation (4) is difficult to solve when $\sigma(x)$ is a variable with x.

In order to effectively analyze the vibration characteristics of beams under nonuniform prestress, a discrete vibration analysis method is proposed in this paper based on the vibration analysis of beams subjected to uniformly distributed prestress. The connection between each segment is established according to the continuity of beams. The method can be applied to the bending vibration analysis of beams under multiple boundary conditions.

According to equations (6) and (7), the beam natural frequencies can be obtained through simple calculation when it is subjected to axial uniform prestress. Then, the corresponding vibration mode function can be obtained. Therefore, the beam with nonuniform prestress is discretized into multiple segments. When the beam is divided into enough segments, each segment can be approximately regarded as being uniformly prestressed.

Without loss of generality, the beam with length L is divided into N segments, each of which is $l=L/N$, as is shown in Figure 1. Actually, the length of each segment of beam is not necessarily L/N, which can be divided according to the actual stress distribution form. The jth segment is taken as the analysis object. The uniform prestress of the segment is set as σ_j. The length of the jth segment is $l_j=l=L/N$. The coordinate of the initial point of jth segment in the global coordinate system is x_{j-1}, and the coordinate of the final point in the global coordinate system is x_j, i.e., $x\in[x_{j-1},x_j]$. The corresponding vibration mode function can be expressed as follows:

$$W_j(x)=a_j\cosh s_{1,j}\left(x-x_{j-1}\right)+b_j\sinh s_{1,j}\left(x-x_{j-1}\right)+c_j\cos is_{2,j}\left(x-x_{j-1}\right)+d_j\sin is_{2,j}\left(x-x_{j-1}\right), \quad (8)$$

where $s_{1,j}^2,s_{2,j}^2=(\sigma_jA/2EI)\pm\sqrt{(\sigma_jA/2EI)^2+(\rho A\omega^2/EI)}$. ω is the natural frequency of the whole beam with length L. $x_0=0$, $x_N=L$.

Similarly, the corresponding mode function of $(j+1)$th segment of the beam can be expressed as

$$W_{j+1}(x)=a_{j+1}\cosh s_{1,j+1}\left(x-x_j\right)+b_{j+1}\sinh s_{1,j+1}\left(x-x_j\right)+c_{j+1}\cos is_{2,j+1}\left(x-x_j\right)+d_{j+1}\sin is_{2,j+1}\left(x-x_j\right), \quad (9)$$

where $x\in[x_j,x_{j+1}]$, $s_{1,j+1}^2,s_{2,j+1}^2=(\sigma_{j+1}A/2EI)\pm\sqrt{(\sigma_{j+1}A/2EI)^2+(\rho A\omega^2/EI)}$.

According to the continuity of the beam, the displacement, rotation angle, bending moment, and shear stress of the beam in the jth and the $(j+1)$th sections at the joint point x_j are equal [20], which is shown in the following equations:

$$W_j\left(x_j\right)=W_{j+1}\left(x_{j+1}\right), \quad (10)$$

$$W_j'\left(x_j\right)=W_{j+1}'\left(x_{j+1}\right), \quad (11)$$

$$W_j''\left(x_j\right)=W_{j+1}''\left(x_{j+1}\right), \quad (12)$$

$$W_j^{(3)}\left(x_j\right)=W_{j+1}^{(3)}\left(x_{j+1}\right). \quad (13)$$

Equation (14) can be obtained by substituting equations (8) and (9) into equations (10)~(13):

$$B_{(j+1)}=Z_j*B_{(j)}, \quad (14)$$

where $B_{(j)}=[a_j,b_j,c_j,d_j]$, $B_{(j+1)}=[a_{j+1},b_{j+1},c_{j+1},d_{j+1}]$.

$$Z_j=\begin{bmatrix} m_1n_1 & m_1n_2 & m_2n_3 & m_2n_4 \\ \frac{s_{1,j}}{s_{1,j+1}}m_1n_2 & \frac{s_{1,j}}{s_{1,j+1}}m_1n_1 & -\frac{i*s_{2,j}}{s_{1,j+1}}m_2n_4 & \frac{i*s_{2,j}}{s_{1,j+1}}m_2n_3 \\ -m_4n_1 & -m_4n_2 & -m_3n_3 & -m_3n_4 \\ -\frac{s_{1,j}}{i*s_{2,j+1}}m_4n_2 & -\frac{s_{1,j}}{i*s_{2,j+1}}m_4n_1 & \frac{s_{2,j}}{s_{2,j+1}}m_3n_4 & -\frac{s_{2,j}}{s_{2,j+1}}m_3n_2 \end{bmatrix}, \quad (15)$$

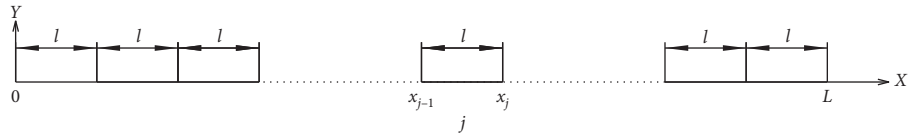

Figure 1: Section diagram of the beam.

where

$$m_1 = \frac{s_{1,j}^2 - s_{2,j+1}^2}{s_{1,j+1}^2 - s_{2,j+1}^2},$$

$$m_2 = \frac{s_{2,j}^2 - s_{2,j+1}^2}{s_{1,j+1}^2 - s_{2,j+1}^2},$$

$$m_3 = \frac{s_{2,j}^2 - s_{1,j+1}^2}{s_{1,j+1}^2 - s_{2,j+1}^2},$$

$$m_4 = \frac{s_{1,j}^2 - s_{1,j+1}^2}{s_{1,j+1}^2 - s_{2,j+1}^2}, \tag{16}$$

$$n_1 = \cosh\, s_{1,j} l_j,$$

$$n_2 = \sinh\, s_{1,j} l_j,$$

$$n_3 = \cos\left(i * s_{2,j} l_j\right),$$

$$n_4 = \sin\left(i * s_{2,j} l_j\right).$$

Therefore, the relationship between $B_{(1)}$ and $B_{(N)}$ can be obtained as

$$B_{(N)} = Z * B_{(1)}, \tag{17}$$

where $Z = Z_{N-1} Z_{N-2} \ldots Z_2 Z_1$ can be obtained according to equation (15).

According to equation (17), the coefficients of the vibration mode function of both 1st and Nth segment of the beam can be represented by $B_{(1)} = [a_1,\ b_1,\ c_1,\ d_1]$. Therefore, the equation about the coefficients $B_{(1)}$ can be obtained by substituting the boundary conditions at both ends of the beam corresponding to $x = 0$ and $x = L$ into the mode function equation (8):

$$\Gamma * B_{(1)} = 0, \tag{18}$$

where the matrix Γ is obtained according to the boundary conditions at both ends of the beam and contains the parameter ω (natural frequency).

Since there must be a mode function of the beam, $B_{(1)} \neq 0$. To make equation (18) true, the determinant of Γ should be zero, which is shown in the following equation:

$$|\Gamma| = 0. \tag{19}$$

According to equation (19), the natural frequencies ω of beam with corresponding constraint form under axial nonuniform prestress can be obtained. The coefficients of the vibration mode functions of 1st segment of the beam can be obtained by substituting the obtained natural frequencies into equation (18). Then, the vibration mode function of 1st segment of the beam can be determined. The vibration mode functions of each segment of the beam can be obtained by substituting $B_{(1)}$ into equation (14). Therefore, the vibration mode functions of the whole beam with corresponding constraint form can be obtained under axial nonuniform prestress.

3. Verification of the Correctness of the Proposed Method

In order to verify the correctness of the method proposed in this paper, a simply supported beam subjected to axial uniform prestress is taken as the analysis object, and the calculation results of the proposed method are compared with those of the traditional method [11, 21] which is employed to analyze the uniformly prestressed beams.

The calculation formula of natural frequencies for transverse vibration of simply supported beam under axial uniform stress is given in reference [11, 21], i.e.,

$$\omega_n = \frac{\pi^2}{L^2} \sqrt{\frac{EI}{\rho A}} \left(n^4 + \frac{n^2 P L^2}{\pi^2 EI} \right)^{1/2}, \tag{20}$$

where L is the total length of the beam, P is the axial tensile force, and n indicates the order of the natural frequency ($n = 1,\ 2,\ 3, \ldots$).

The beam is divided into two sections, each with a length of 0.5 l. Each section is subjected to uniform prestress $\sigma_j = (P/A)\,(j = 1,\ 2)$. The natural frequencies are calculated with the method proposed in this paper and the traditional method, respectively.

The boundary conditions at both ends of the simply supported beam are zero displacement and bending moment, i.e.,

$$\begin{cases} W_1(0) = 0, \\ W_1''(0) = 0, \\ W_N(L) = 0, \\ W_N''(L) = 0, \end{cases} \tag{21}$$

where $N = 2$ since the beam is divided into 2 sections.

Equations (8) and (9) are substituted into equation (21), which is shown in the following equations:

$$\begin{bmatrix} 1 & 0 & 1 & 0 \\ s_{11}^2 & 0 & s_{21}^2 & 0 \end{bmatrix} \begin{bmatrix} a_1 \\ b_1 \\ c_1 \\ d_1 \end{bmatrix} = \Gamma_{10} \begin{bmatrix} a_1 \\ b_1 \\ c_1 \\ d_1 \end{bmatrix} = 0, \tag{22}$$

$$\Gamma_{N0} \begin{bmatrix} a_N \\ b_N \\ c_N \\ d_N \end{bmatrix} = 0, \tag{23}$$

where

$$\Gamma_{N0} = \begin{bmatrix} \cosh(s_{1N} l_N) & \sinh(s_{1N} l_N) & \cos(i * s_{2N} l_N) & \sin(i * s_{2N} l_N) \\ s_{1N}^2 \cosh(s_{1N} l_N) & s_{1N}^2 \sinh(s_{1N} l_N) & s_{2N}^2 \cos(i * s_{2N} l_N) & s_{2N}^2 \sin(i * s_{2N} l_N) \end{bmatrix}. \tag{24}$$

Then, equation (17) is substituted into equation (23) to obtain matrix Γ, which consists of Γ_1 and Γ_N:

$$\begin{bmatrix} \Gamma_1 \\ \Gamma_N \end{bmatrix} \begin{bmatrix} a_1 \\ b_1 \\ c_1 \\ d_1 \end{bmatrix} = \Gamma \begin{bmatrix} a_1 \\ b_1 \\ c_1 \\ d_1 \end{bmatrix} = 0, \tag{25}$$

where $\Gamma_1 = \Gamma_{10}$, $\Gamma_N = \Gamma_{N0} \cdot Z$.

Therefore, the natural frequencies can be obtained according to equation (19).

The specific parameters take $l = 1$ m, $\rho = 7830$ kg/m^3, $E = 2.19 \times 10^{11}$ Pa, $\mu = 0.3$, $d = 0.02$ m, and $P = 1000$ N. The calculation results are shown in Table 1.

As shown in Table 1, when two decimal places are retained, the errors of the first four orders natural frequencies calculated by the method proposed in this paper and the method in reference [11, 21] are 0.00.

To further illustrate the correctness of the method, an experiment was carried out. The first-order natural frequency of a beam with a diameter of 0.006 m was tested under different axial tensile force. The material of the beam was SUS303. The test length of the beam was 0.51 m. The force hammer, laser accelerometer, and tension machine were used for excitation, signal acquisition, and application of axial tensile force, respectively. The axial tensile force was firstly acted by the tension machine. After the axial tensile force was stable, the beam was hammered and the acceleration signal was collected by laser accelerometer. The $m + p$ international SO Analyzer was used to signal collection (used in conjunction with laser accelerometer) and analysis. The test device is shown in Figure 2. The results are obtained as Table 2 and Figure 3. According to the results of analysis and experiment, the correctness of the method proposed in this paper can be verified.

4. Bending Vibration Analysis of a Nonuniformly Prestressed Ball Screw

Based on the proposed method, the quasistatic analysis of a tensioned ball screw during the cutting process is carried out, i.e., the axial force applied on the ball screw is a constant during analysis.

During analysis, both ends of the ball screw are fixed and there is a prestretch of $L' - L$ in the ball screw, resulting in prestress σ_0. In order to simplify the analysis, the ball screw is simplified to a cylindrical beam. Meanwhile, the influence of the prestretch $L' - L$ on the total length L is ignored since $L' - L$ is much smaller than L. In this paper, only the effect of the axial force on the vibration characteristics of ball screw is considered because the ball screw only constrains the degree of freedom of the axial translation of the slide table. In general, only one slide table is installed on the ball screw for mounting the tool holder. Therefore, the ball screw is divided into two sections, and it is considered that each section of ball screw is uniformly stressed, respectively, in this paper. The simplified model is shown in Figure 4, and the three-dimensional model of the linear guideway and ball screw system is shown in Figure 5.

Under the hypothesis of small amplitude vibrations, it is neglected the constraint constituted by the slide guide for the presence of backlash. The transversal component of the cutting force is therefore not absorbed by the slide guide. Consequently, the boundary conditions at both ends of the simplified model shown in Figure 4 are that both the displacement and the rotation angle are zero.

$$\begin{cases} W_1(0) = 0, \\ W_1'(0) = 0, \\ W_N(L) = 0, \\ W_N'(L) = 0. \end{cases} \tag{26}$$

Therefore, matrix Γ can be obtained similar to Section 2, which is shown as

$$\Gamma = \begin{bmatrix} \Gamma_1 \\ \\ \Gamma_N \end{bmatrix} = \begin{bmatrix} \Gamma_{10} \\ \\ \Gamma_{N0} \cdot Z \end{bmatrix}, \tag{27}$$

where

Table 1: Comparison of calculation results of natural frequencies of simply supported beam under axially uniform prestress between two methods.

Order	Calculation results of natural frequencies (Hz)		Error
	This paper	Reference [11, 21]	
1	42.74	42.74	0.00
2	167.37	167.37	0.00
3	375.05	375.05	0.00
4	665.81	665.81	0.00

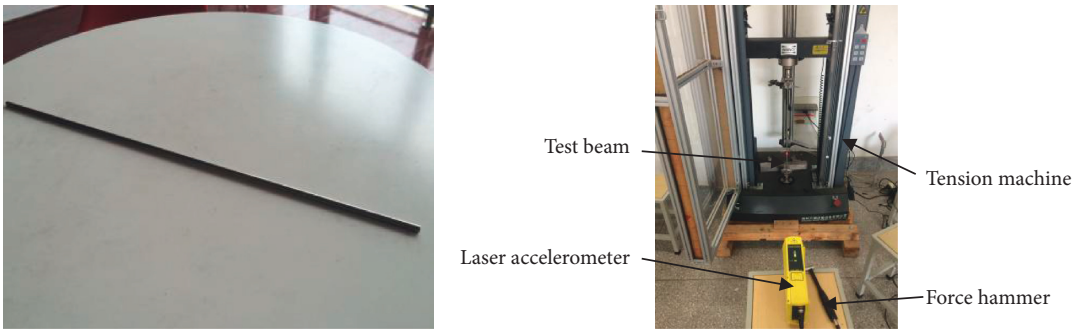

(a) (b)

Figure 2: The natural frequency test of the prestressed beam. (a) The test beam. (b) The test device.

Table 2: First-order natural frequency of the beam under different axial tensile forces.

Axial tensile force (N)	First-order natural frequency (Hz)		Error (%)
	This paper	Experiment	
0	45.49	44.5	2.18
265	56.62	55.5	1.98
505	65.07	66	−1.43
775	73.43	75	−2.14
1005	79.86	81	−1.43

$$\Gamma_{10} = \begin{bmatrix} 1 & 0 & 1 & 0 \\ 0 & s_{11} & 0 & i * s_{21} \end{bmatrix},$$
$$\Gamma_{N0} = \begin{bmatrix} \cosh(s_{1N} l_N) & \sinh(s_{1N} l_N) & \cos(i * s_{2N} l_N) & \sin(i * s_{2N} l_N) \\ s_{1N} \sinh(s_{1N} l_N) & s_{1N} \cosh(s_{1N} l_N) & -i * s_{2N} \sin(i * s_{2N} l_N) & i * s_{2N} \cos(i * s_{2N} l_N) \end{bmatrix}, \tag{28}$$

where

$$N = 2, s_{1,j}^2, s_{2,j}^2 = \frac{\sigma_j A}{2EI} \pm \sqrt{\left(\frac{\sigma_j A}{2EI}\right)^2 + \frac{\rho A \omega^2}{EI}}, \quad j = 1,\ 2. \tag{29}$$

The natural frequencies of the transverse vibration of the ball screw can be obtained by substituting equation (27) into equation (19). Then, the proportional relationship between a_1, b_1, c_1, and d_1 can be obtained according to equation (26), and $B_{(2)} = [a_2,\ b_2,\ c_2,\ d_2]$ can also be obtained according to equations (17) and (30). Moreover, the vibration mode function of the ball screw can be achieved according to $B_{(1)}$ and $B_{(2)}$, which is shown as

$$a_1 : b_1 : c_1 : d_1 = 1 : \frac{\Gamma(3,1) - \Gamma(3,3)}{\Gamma(3,2) - (s_{11}/i * s_{21})\Gamma(3,4)} : -1 : \frac{s_{11}}{i * s_{21}} \frac{\Gamma(3,1) - \Gamma(3,3)}{\Gamma(3,2) - (s_{11}/i * s_{21})\Gamma(3,4)}, \tag{30}$$

$$W(x) = \begin{cases} a_1 \cosh s_{1,1}(x - x_0) + b_1 \sinh s_{1,1}(x - x_0) + c_1 \cos i s_{2,1}(x - x_0) + d_1 \sin i s_{2,1}(x - x_0), & 0 \le x \le l_1, \\ a_2 \cosh s_{1,2}(x - x_1) + b_2 \sinh s_{1,2}(x - x_1) + c_2 \cos i s_{2,2}(x - x_1) + d_2 \sin i s_{2,2}(x - x_1), & l_1 \le x \le L, \end{cases} \tag{31}$$

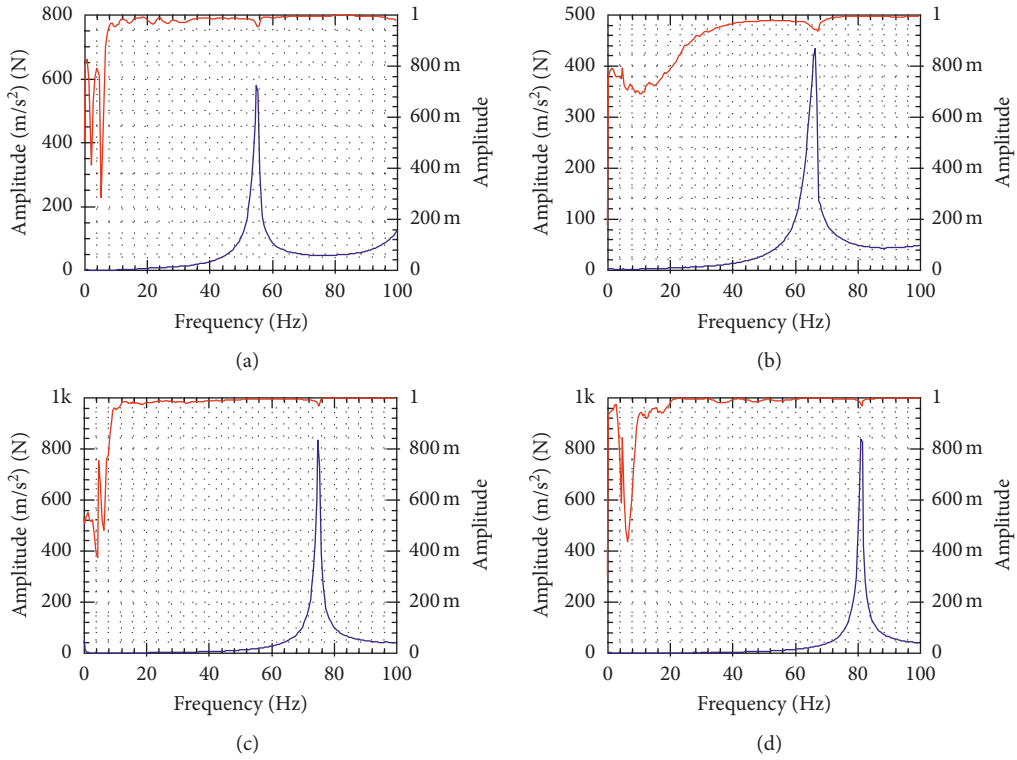

Figure 3: The test results of the beam under different axial tensile forces (solid line: frequency response function; dotted line: coherence function). (a) $F = 265$ N. (b) $F = 505$ N. (c) $F = 775$ N. (d) $F = 1005$ N.

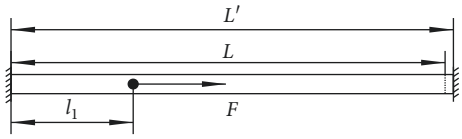

Figure 4: Simplified model of the ball screw.

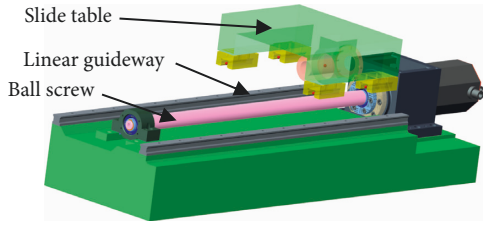

Figure 5: Three-dimensional model of the linear guideway and ball screw system.

where $x_0 = 0$, $x_1 = l_1$.

The following typical ball screw parameters are taken to analyze $l = 1$ m, $\rho = 7830$ kg/m^3, $E = 2.19 \times 10^{11}$ Pa, $\mu = 0.3$, $d = 0.02$ m, and $L' - L = 0.04$ mm. The natural frequencies of ball screw with predeformation are calculated, as is shown in Table 3. The effect of the predeformation on the first-order natural frequency is shown in Figure 6.

According to Table 3 and Figure 6, it can be seen that prestress has certain influence on the natural frequencies of the ball screw. The first-order natural frequency of the ball screw increases with the increase of the predeformation.

Table 3: Natural frequencies of ball screw with predeformation.

Order	Frequency (Hz)		
	Nonstress	Prestretching $L' - L = 0.04$ mm	Difference
1	94.16	95.99	1.83
2	259.55	262.05	2.5
3	508.83	511.57	2.74
4	841.12	844	2.88

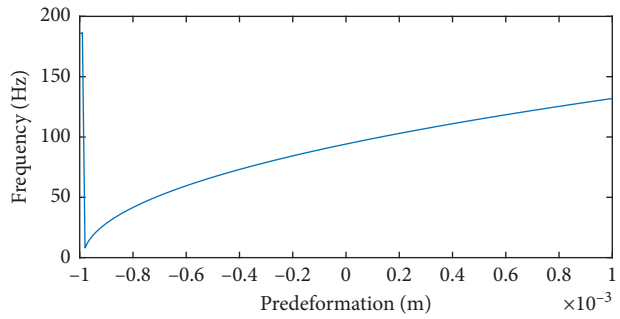

Figure 6: Effect of the predeformation on the first-order natural frequency.

The natural frequency presents a power level change $f = a \cdot (\Delta L + b)^{1/2}$ with the change of predeformation ΔL, which is consistent with the relationship between angular frequency and stress in reference [16]. A sudden change occurs when ΔL approaches -1×10^{-3} m in Figure 6. This phenomenon is due to the instability of the ball screw.

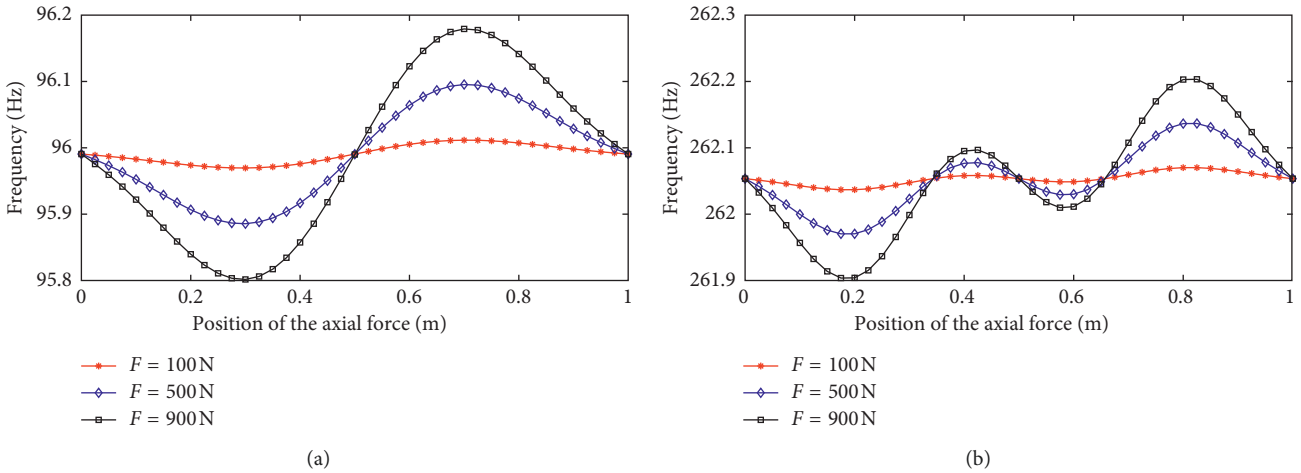

Figure 7: Influence of the location and amplitude of the axial force on natural frequencies of the ball screw. (a) First-order natural frequency. (b) Second-order natural frequency.

In fact, for the beam structure with fixed supports at both ends, the critical force of its instability is shown in the following equation [22] when subjected to pressure:

$$F_{cr} = \frac{\pi^2 EI}{(0.5L)^2}, \tag{32}$$

where L is the total length of the beam.

It can be obtained that the critical force of the ball screw analyzed in this paper is $F_{cr} = 67904$ N by substituting the parameters into equation (32). The corresponding pre-deformation is -9.8696×10^{-4} m, which is consistent with the mutation phenomenon in Figure 6.

Furthermore, the influence of the location and amplitude of the axial force on natural frequencies of ball screw is researched. The first two natural frequencies of the ball screw corresponding to different locations and amplitudes of the axial force are calculated as shown in Figure 7.

As shown in Figure 7, the first two natural frequencies show a trend of simple harmonic variation with the movement of the force point from $x = 0$ to $x = L$, where the direction from $x = 0$ to $x = L$ is the direction of force F. The period of second-order frequency is twice that of first-order frequency. The force F has almost no influence on the natural frequencies of the ball screw as the force position at the centre point of the screw. Moreover, the greater the force, the greater the change in natural frequency.

The first-order natural frequency will affect the development of the maximum speed of the ball screw (generally, the speed of the ball screw must be lower than 80% of the first critical speed to avoid severe bending vibrations). Therefore, the influence of the cutting force on the first-order natural frequency of the ball screw is further studied. The first-order natural frequencies under different forces are calculated when the force position is 0.3 L as shown in Figure 8. The results show that the natural frequency decreases with the increase of the applied force. According to equation (2), the natural frequencies of ball screw are actually directly related to stress in the ball screw. Meanwhile, the diameter of the ball screw will influence its stress. Hence, the change rate of

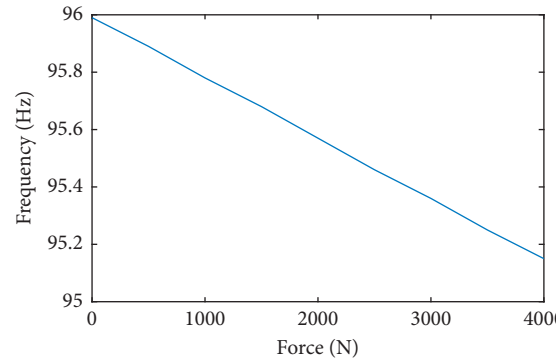

Figure 8: First natural frequencies of ball screw under different forces ($d = 0.02$ m, force position is 0.3 L).

first natural frequency with an axial component of the cutting force (1000 N) relative to that without cutting force for different diameters of ball screw is calculated as shown in Figure 9. According to Figure 9, the change rate of the first natural frequency exceeds 20% when the diameter is less than 0.006 m. The results further illustrate that the greater the stress in the ball screw, the greater the change in natural frequency. Consequently, the cutting force will reduce the screw transversal stiffness when the force point is in some positions. In some cases, it is even possible that the first critical speed can be reached during operation.

5. Instantaneous Frequency of Tensioned Ball Screw during the Cutting Process

In the fourth section, quasistatic analysis of ball screw is carried out. However, the axial force applied on the ball screw changes at all times during machining. Therefore, the natural frequencies also vary with the axial force.

In order to research the instantaneous frequencies of tensioned ball screw during the cutting force, a surfacing machining process is carried out to obtain the typical varying axial cutting force. Then, the data are employed to calculate

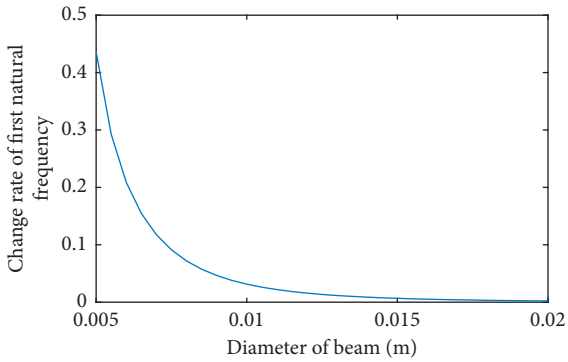

Figure 9: Change rate of first natural frequency at different diameters.

Table 4: Processing parameters of the process.

Spindle speed	Feed rate	Cutting quantity (one side)	Workpiece material
1000 r/min	300 mm/min	1 mm	45#

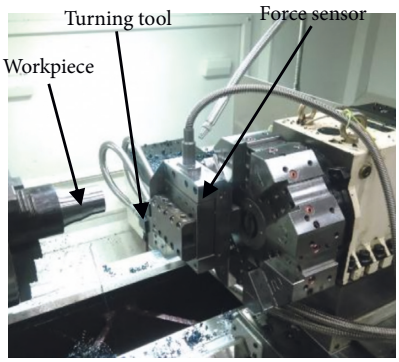

Figure 10: Surfacing machining process.

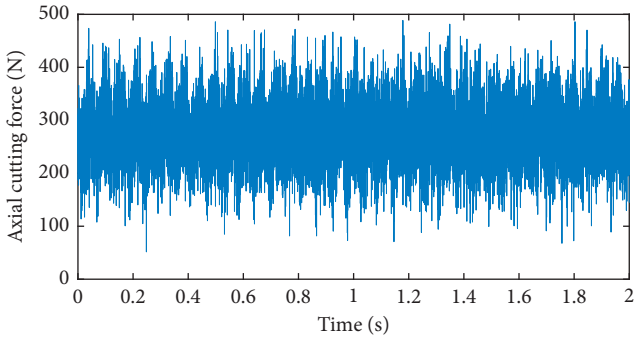

Figure 11: Time domain signal of axial cutting force.

the instantaneous frequencies based on the method proposed in this paper. The processing parameters of the process are shown in Table 4. The axial cutting force is acquired by Kistler9129AA, as shown in Figure 10. 2-second cutting force data in stable machining state are intercepted in the paper, and the time domain signal is shown in Figure 11.

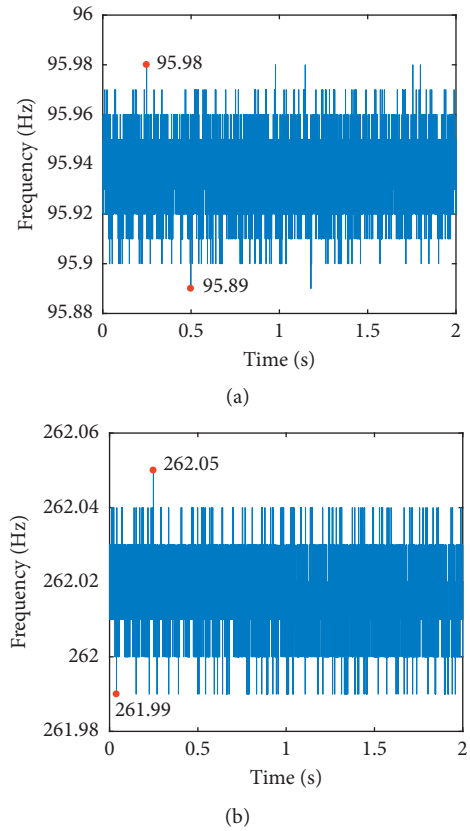

Figure 12: First two instantaneous frequencies of tensioned ball screw during the cutting process.

As the ball screw constrains the degree of freedom of the axial translation of the slide table while the linear guideway constrains the other five degrees of freedom of the slide table; it is easy to analyze that the axial force applied on the ball screw is equal to the axial cutting force applied on the cutting tool. Then, according to the data obtained by the test, the first two instantaneous frequencies of tensioned ball screw are calculated with the initial location of the force in $x = 0.25\ L$. The results are shown in Figure 12.

According to Figure 12, the axial cutting force has certain influence on the natural frequencies of the tensioned ball screw. The maximum natural frequency of the first order is 95.89 Hz while the minimum natural frequency of the first order is 95.89 Hz. The influence of the axial cutting force will be greater when the axial cutting force is greater or the ball screw stiffness is lower. Therefore, the frequency range should be taken into account in the design process rather than simply considering the frequency without prestress.

6. Conclusion

In this study, to investigate the influence of the cutting process on the natural frequency of tensioned ball screw, a new method to analyze the bending vibration of a beam under nonuniform prestress is proposed. This method is suitable for vibration analysis of beams under different boundary conditions. The numerical results show that axial

force applied on the ball screw produced in the cutting process has a certain influence on the dynamic characteristics of the ball screw. A surfacing machining process is carried out, and the cutting force data are obtained to calculate the instantaneous frequency of ball screw. According to the research in this paper, the frequency range should be considered in the design process of ball screws and machine tools.

Data Availability

The data used to support the findings of this study are available from the corresponding author upon request.

Conflicts of Interest

The authors declare that there are no conflicts of interest regarding the publication of this paper.

Acknowledgments

This work was supported by the National Science and Technology Major Project (Approval nos. 2013ZX04012032 and 2012ZX04002032) and 2017 Science and Technology Support Plan of Nanjing Jiangsu China (Approval no. 201701213).

References

[1] Y. Altintas, A. Verl, C. Brecher, L. Uriarte, and G. Pritschow, "Machine tool feed drives," *CIRP Annals*, vol. 60, no. 2, pp. 779–796, 2011.

[2] Y. H. Choi, S. M. Cha, J. H. Hong, and J. H. Choi, "A study on the vibration analysis of a ball screw feed drive system," *Materials Science Forum*, vol. 471-472, pp. 149–154, 2004.

[3] L. Zhang, T. Wang, S. Tian, and Y. Wang, "Analytical modeling of a ball screw feed drive for vibration prediction of feeding carriage of a spindle," *Mathematical Problems in Engineering*, vol. 2016, Article ID 2739208, 8 pages, 2016.

[4] D. Wang, Y. Lu, T. Zhang, K. Wang, and A. Rinoshika, "Effect of stiffness of rolling joints on the dynamic characteristic of ball screw feed systems in a milling machine," *Shock and Vibration*, vol. 2015, Article ID 697540, 11 pages, 2015.

[5] S. Jiang and S. L. Zhu, "Dynamic characteristic parameters of linear guideway joint with ball screw," *Journal of Mechanical Engineering*, vol. 46, no. 1, pp. 92–99, 2010.

[6] C. Y. Lin, J. P. Hung, and T. L. Lo, "Effect of preload of linear guides on dynamic characteristics of a vertical column–spindle system," *International Journal of Machine Tools and Manufacture*, vol. 50, no. 8, pp. 741–746, 2010.

[7] J.-P. Hung, Y.-L. Lai, C.-Y. Lin, and T.-L. Lo, "Modeling the machining stability of a vertical milling machine under the influence of the preloaded linear guide," *International Journal of Machine Tools and Manufacture*, vol. 51, no. 9, pp. 731–739, 2011.

[8] H.-W. Huang, M.-S. Tsai, and Y.-C. Huang, "Modeling and elastic deformation compensation of flexural feed drive system," *International Journal of Machine Tools and Manufacture*, vol. 132, pp. 96–112, 2018.

[9] F. Li, Y. Jiang, T. Li, and K. F. Ehmann, "Compensation of dynamic mechanical tracking errors in ball screw drives," *Mechatronics*, vol. 55, pp. 27–37, 2018.

[10] N. Bideau, L. Le Marrec, and L. Rakotomanana, "Influence of a finite strain on vibration of a bounded Timoshenko beam," *International Journal of Solids and Structures*, vol. 48, no. 16-17, pp. 2265–2274, 2011.

[11] N. Ashwear and A. Eriksson, "Natural frequencies describe the pre-stress in tensegrity structures," *Computers & Structures*, vol. 138, pp. 162–171, 2014.

[12] F. J. Nieves, A. Bayón, F. Gascón, R. Medina, and F. Salazar, "Nonlinear bending vibration of a prestressed thick plate," *Journal of Mechanical Science and Technology*, vol. 32, no. 4, pp. 1505–1517, 2018.

[13] M. T. Kashani, S. Jayasinghe, and S. M. Hashemi, "Dynamic finite element analysis of bending-torsion coupled beams subjected to combined axial load and end moment," *Shock and Vibration*, vol. 2015, Article ID 471270, 12 pages, 2015.

[14] H. Zhang, H. Yuan, W. Yang, and T. Zhao, "Vibration reduction optimization of the mistuned bladed disk considering the prestress," *Proceedings of the Institution of Mechanical Engineers, Part G: Journal of Aerospace Engineering*, vol. 233, no. 1, pp. 226–239, 2019.

[15] Z. Li, W. Yang, and H. Yuan, "Vibration analysis of aero-engine blisk structure based on a prestressed CMS super-element method," *Shock and Vibration*, vol. 2016, Article ID 1021402, 10 pages, 2016.

[16] L. Li and L. Chen, "Parametric instability analysis of the top-tensioned riser in consideration of complex pre-stress distribution," *Advances in Mechanical Engineering*, vol. 10, no. 1, article 168781401775389, 2018.

[17] J. Li, "Effect of pre-stress on natural vibration frequency of the continuous steel beam based on Hilbert-Huang transform," *Journal of Vibroengineering*, vol. 18, no. 5, pp. 2818–2827, 2016.

[18] Z. Zhang, D. Zhang, M. Luo, and B. Wu, "Research of machining vibration restraint method for compressor blade," *Procedia CIRP*, vol. 56, pp. 133–136, 2016.

[19] M. Wan, T.-Q. Gao, J. Feng, and W.-H. Zhang, "On improving chatter stability of thin-wall milling by prestressing," *Journal of Materials Processing Technology*, vol. 264, pp. 32–44, 2019.

[20] C. Cui, H. Jiang, and Y. H. Li, "Semi-analytical method for calculating vibration characteristics of variable cross-section beam," *Journal of Vibration and Shock*, vol. 31, no. 14, pp. 85–88, 2012.

[21] S. S. Rao, X. Y. Li, and M. L. Zhang, *Mechanical Vibration*, Tsinghua University, Beijing, China, 2009.

[22] H. W. Liu, *Mechanics of Materials I*, Higher Education Press, Beijing, China, 2011.